Indonesian Journal of Material Research
***e*-ISSN: 2987-1654**
Vol. 1, No. 2, July 2023

Indonesian Journal of MATERIAL RESEARCH

Research Paper

Adsorption of Phenol using Cellulose and Hydrochar: Kinetic, Isotherm, and Regeneration Studies

Sahrul Wibiyan[1]*, Alfan Wijaya[1], Patimah Mega Syah Bahar Nur Siregar[1]

[1] *Research Center of Inorganic Materials and Coordination Complexes, Sriwijaya University, Palembang, South Sumatera, 30139, Indonesia*
***Corresponding author**: sahrulwib@gmail.com

Abstract
In this study, hydrocarbons were obtained through the hydrothermal carbonization synthesis method. The XRD data of the cellulose sample revealed 2θ angles of 15.46°, 22.34°, and 34.36°, indicating that the cellulose sample under investigation had an amorphous structure. The XRD data of the hydrocarbon sample showed a 2θ angle of 25.72°, indicating the presence of graphitic carbon. The FTIR spectra of both cellulose and hydrocarbon exhibited similarities at wave numbers 3394 cm^{-1}, 2893 cm^{-1}, 1662 cm^{-1}, 1000-1200 cm^{-1}, and 847 cm^{-1}. BET analysis revealed that the hydrocarbon material surface area measured was 7.366 m^2/g, measured pore volume for the entire sample was 0.008 cc/g, and the average size of the pores was 3.189 nm. The optimal pH variation for cellulose was at pH 10, with an adsorption capacity of 10.75 mg/g, on the other hand, was tested at pH 6 and demonstrated an adsorption capacity of 12.74 mg/g. The adsorption kinetics model for both adsorbents was PSO, and the adsorption isotherm model was Freundlich. Cellulose exhibited a maximum adsorption capacity of 35.336 mg/g, while hydrochar demonstrated a maximum adsorption capacity of 21.008 mg/g. It is noteworthy that both adsorbents were capable of being reused for up to five cycles.

Keywords
Adsorption, Phenol, Cellulose, Hydrochar, Kinetic

Received: 13 May 2023, Accepted: 16 July 2023
https://doi.org/10.26554/ijmr.2023129

1. INTRODUCTION

Phenol, an hazardous organic contaminant, has the potential to enter and pollute surface water as a result of industrial wastewater discharge from sectors such as pharmaceuticals, petrochemicals, dyes, and pesticides (Gao et al., 2021; Fang et al., 2021; Zhang et al., 2019). The existence of phenol in the environment, especially in water, can cause significant harm to aquatic ecosystems and present risks to human well-being and safety (da Silva et al., 2022). To ensure the safety of water sources, the United States Environmental Protection Agency (USEPA) has established a permissible level of 1 microgram per liter (μg/L) for phenol. According to de Farias et al. (2022), this restriction is intended to regulate and control the amount of phenol in water and ensure its safety for a variety of uses. In fact, phenol is regarded as an environmentally dangerous chemical since it has carcinogenic and poisonous qualities that endanger both human health and ecological systems. Phenol in the environment, especially in water bodies, can have negative effects on aquatic life and the health of the entire ecosystem. Therefore, it is crucial to establish efficient management methods and practical countermeasures to phenol contamination. The protection of human health and wellbeing as well as the preservation of the ecosystem depend on such measures (Chaari et al., 2021).

Adsorption is acknowledged as an effective and affordable approach for phenol elimination. It has various benefits, including as reduced emissions of secondary pollutants, low energy usage, and the potential for recurrent use of the adsorbents. Adsorption can thus be a sustainable and eco-friendly method of phenol contamination water treatment (Sajid et al., 2018). The removal of phenolic compounds can be accomplished using a variety of adsorbents. Examples include hemitatite composite (Dehmani et al., 2023b), Chitosan (Utami et al., 2022) and activated carbon made from oak wood (Dehmani et al., 2023a). These adsorbents have been investigated and have demonstrated potential for efficiently adsorbing phenolic chemicals, providing interesting possibilities for phenol removal in a variety of applications.

The strong chemical stability, porous structure, physical and chemical characteristics, and significant surface area of carbon-based compounds, such as hydrochar, are well known. Because of their exceptional stability, these materials will perform and last in a variety of applications. Increased adsorption capacity and accessibility to target molecules or contaminants are made possible by the presence of a porous structure. In addition, they exhibit attractive qualities for particular applications,

including adsorption, catalysis, and energy storage, because to their distinct physical and chemical properties. Additionally, carbon-based materials are adaptable and helpful in a variety of disciplines due to their considerable surface area, which allows for ample room for interactions with other chemicals (Zulfajri et al., 2021).

In this investigation, hydrothermal carbonization was used to create hydrocharbon. Utilizing Fourier Transform Infrared (FTIR) spectroscopy and X-Ray Diffraction (XRD) analysis, the materials obtained for cellulose and hydrochar were examined. The crystalline structure of the materials can be examined, and the phases present in the material can be identified, using XRD analysis. By examining their vibrational modes, FTIR spectroscopy is used to locate and investigate the functional groups present in the materials. Understanding the structural and chemical features of cellulose and hydrochar materials is aided by these approaches, which also reveal some of their potential uses. To ascertain the materials' surface area and pore characteristics, including pore volume and pore size distribution, BET analysis is used. These characterisation methods provide useful perceptions into the structural, chemical, and biological

2. EXPERIMENTAL SECTION

2.1 Chemical and Instrumental

The experimental setup included the use of analytical grade substances such as phenol (C_6H_5OH), distilled water (H_2O), 4-aminoantipyrine ($C_{11}H_{13}N_3O$), cellulose, potassium hexacyanoferrate(III) ($K_3[Fe(CN)_6]$), sodium acetate buffer solution (CH_3COONa) with a pH of 10, hydrochloric acid (HCl), and sodium hydroxide (NaOH). Hydrothermal carbonization was employed to produce the hydrochar used in the experiment. The following instruments were used to characterize the adsorbents: Rigaku Miniflex-6000 X-ray diffractometer, Shimadzu Prestige-21 Fourier transform infrared spectrometer, Surface Area Analyzer-Brunauer Emmet Teller (BET) model NOVA 4200e, and Biobase BK-UV 1800 PC spectrophotometer. These equipment were used to examine the properties of the adsorbents, such as their crystal structure, functional groups, surface area, and absorbance.

2.2 Adsoprtion of Phenol

The phenol complex was created by adding 1 mL of a 5 mg/L phenol solution to a beaker. This was done to help in the analysis of phenol using a UV-VIS spectrophotometer. The addition of the solution led in the creation of a colorful complex, making the phenol content more apparent and easier to detect and measure precisely (Xie et al. 2020). Spectrophotometry was used to evaluate phenol, with a 4-aminoantipyrine reagent added. The reaction between phenol and 4-aminoantipyrine results in the synthesis of quinoneimine, which results in the formation of a reddish-brown tint. Under alkaline conditions, the addition of potassium ferricyanide ($K_3Fe(CN)_6$) improves color development (Afifah et al., 2022). 1 mL of phenol solution was carefully transferred into a beaker during the experiment. The beaker was then filled with 0.1 mL of 4-aminoantipyrine 2% solution, 0.1 mL of potassium hexacyanoferrate (III) 8% solution, 1 mL of pH 10 buffer solution, and 3 mL of pure water. The finished mixture was thoroughly stirred to achieve homogeneity before being set aside for 5 minutes to cool. The maximal wavelength for measuring the complexed phenol after incubation was determined to be 510 nm. This wavelength was employed as a point of reference for future investigation and measurement of complexed phenol content.

2.3 Effect of pH Adsorption

A 100 mL beaker was filled with an amount of adsorbent weighing up to 0.05 g. The beaker previously had 50 mL of phenol solution at a concentration of 20 mg/L. The pH of the solution was varied between 2 and 11 (specifically, pH 2, 3, 4, 5, 6, 7, 8, 9, 10, and 11). The mixture was then shaken for 2 hours to enhance adsorption. Following the stirring period, the separation was accomplished using centrifugation. A UV-Vis spectrophotometer was used to measure the unadsorbed phenol in the resultant filtrate. The filtrate was complexed with 4-aminoantipyrine and potassium hexacyanoferrate (III) before to measurement to improve the detectability and measurement accuracy of the phenol concentration.

2.4 Effect of Adsorption Time

The duration of contact between the adsorbate (phenol) and adsorbent was adjusted to investigate the effect of adsorption contact time on the adsorbent. Initially, 0.05 g of the adsorbent was mixed into a 50 mL phenol solution containing 20 mg/L. After stirring the mixture, the adsorption contact time was adjusted at precise intervals of 0, 20, 40, 60, 80, 100, 120, 140, 160, and 180 minutes. The adsorbent was removed from the phenol solution using a separation method after each specified contact time. The solution was then treated with 4-aminoantipyrine and potassium hexacyanoferrate (III) to form a complex, and the complex's absorbance was measured with a UV-Vis spectrophotometer. This technique allowed for the quantification of the phenol concentration in the solution after various contact times with the adsorbent, offering insights into the adsorption process's kinetics.

2.5 Effect of Concentration and Adsorption Temperature

0.05 g of the adsorbent was added to 50 mL of phenol solution at concentrations of 20 mg/L, 30 mg/L, 40 mg/L, 50 mg/L, and 60 mg/L in the experiment. The temperature of the solution was varied to several levels, including 30°C, 40°C, 50°C, and 60°C. After that, the mixture was agitated for 2 hours to allow for adsorption. Following the stirring period, the adsorbent was centrifuged to separate it from the phenol solution. The solution was then treated with 4-aminoantipyrine and potassium hexacyanoferrate (III) to form a complex, and the complex's absorbance was measured using a UV-Vis spectrophotometer. This technique allowed for the quantification of the phenol concentration in the solution at various starting concentrations and temperatures, offering insights into the adsorbent's adsorption capacity and efficiency under various conditions.

3. RESULTS AND DISCUSSION

The X-ray diffraction (XRD) pattern depicting the cellulose and hydrochar is presented in Figure 1. The XRD patterns of cellulose, as shown in Figure 1(a), exhibit prominent peaks at around 15.46°, 22.34°, and 34.36° in the 2θ angles. The presence of these distinct peaks indicates that the cellulose samples being studied possess a characteristic amorphous structure. These diffraction results align with the data provided in ICDD PDF 00-060-1501 (Montoya-Escobar et al., 2022). The hydrochar XRD diffraction shown at Figure 1(b) analysis at 2θ angles revealed the presence of four peaks: 15.48°, 22.54°, 25.72°, and 34.46°. The diffraction peaks observed at 15.48°, 22.54°, and 34.46° can be identified as originating from cellulose. However, the diffraction peak at 2θ 25.72° is identified as graphitic carbon (Yang et al., 2021). Similar to the study conducted by Siregar et al. (2022) the peak at an angle of 22.54° indicating of cellulose.

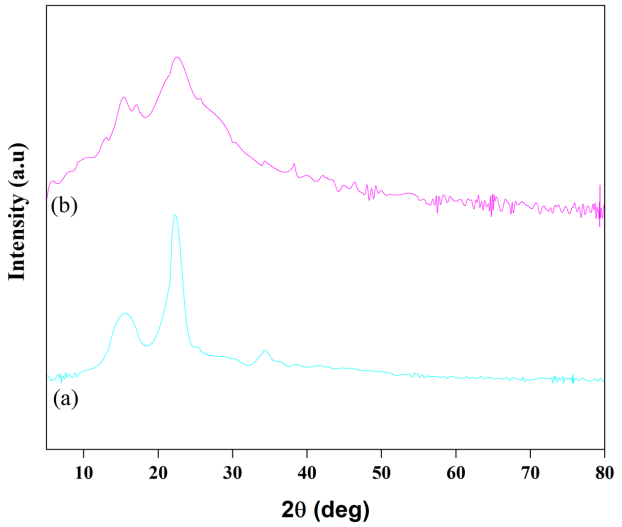

Figure 1. XRD Diffraction of Cellulose (a) and Hydrochar (b)

Figure 2(a) illustrates the FTIR spectrum of cellulose, revealing several distinct peaks. In the vicinity of 3394 cm^{-1}, stretching vibrations of OH groups are prominently observed. Additionally, the peak at 2893 cm^{-1} corresponds to stretching vibrations of C-H groups, while the peak at 1662 cm^{-1} represents stretching vibrations of C-H groups. The presence of a peak at 1635 cm^{-1} indicates the deformation vibration of OH groups in bound water. Moreover, within the range of 1000-1200 cm^{-1}, the FTIR spectrum of cellulose exhibits peaks associated with the stretching of C-O-C and C-O vibrations. The presence of a peak at 847 cm^{-1} in the FTIR spectrum indicates vibrations related to the β-1,4 bonds (Atykyan et al., 2020). Comparatively, the FTIR spectrum of the hydrochar, shown in Figure 2(b), is similar to that of cellulose. This suggests that the hydrochar possesses the same functional groups as cellulose. However, there is a distinguishing peak at 3355 cm^{-1} in the hydrochar, which exhibits a more gradual slope. This indicates a lower concentration of water or O-H bonds, suggesting a reduction in water content due to the carbonization process (Yu et al., 2023).

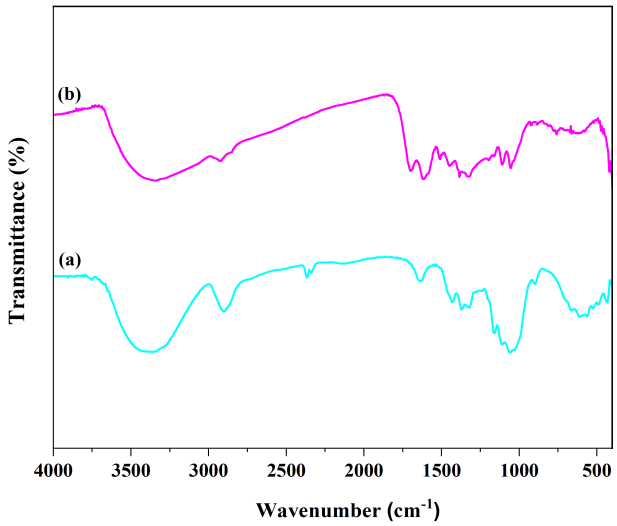

Figure 2. FTIR Spectrum of Cellulose (a) and Hydrochar (b)

BET tests are critical for determining a material's surface area. These tests entail using nitrogen as an adsorbate under liquid nitrogen (77 K) conditions to properly determine the surface area of the material. Scientists can learn a lot about a material's surface properties and its potential for adsorption and other surface-related activities by doing BET tests (Peyrovi and Abolhassanzadeh Parizi, 2022). The adsorption isotherm of the substance utilized as an adsorbent corresponds to a type IV isotherm, according to IUPAC classification (Figure 3). This type of isotherm frequently indicates the presence of mesopores within the material, with pore sizes ranging from 2 to 50 nm. When nitrogen is adsorbed into these mesopores, the pore volume is occupied or filled. This observation sheds light on the porosity and pore structure of the material, notably in the mesopore region (El Hassani et al., 2017). The hydrochar material has a surface area of 7.366 square meters per gram (m^2/g), a total pore volume of 0.008 cubic centimeters per gram (cc/g), and an average pore size of 3.189 nanometers (nm). These properties show the porosity and pore structure of the hydrochar material, emphasizing its adsorption capacity and possible uses in a variety of industries.

The pH of a solution is an important component that has a significant impact on the phenol adsorption processes. It is crucial in defining the availability and reactivity of active sites on the surfaces of activated carbon materials investigated in this study, such as hydrochar and cellulose. Hydrochar and cellulose surfaces are diverse, with both positive and negative sites. The pH of the solution effects phenol ionization and speciation, and thus the surface charge of the adsorbent. This, in turn, regulates the electrostatic interactions between adsorbent and phenol molecules, eventually influencing adsorption behavior and process efficiency. As a result, increasing the adsorption capacity and efficiency of cellulose and hydrochar for phenol removal requires controlling and modifying the pH of the solution

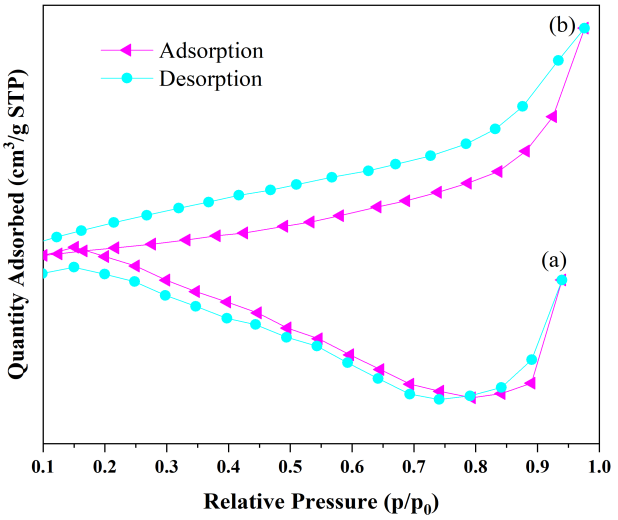

Figure 3. N_2 Adsorption-Desorption Isotherm of Cellulose (a) and Hydrochar (b)

(Mohammad et al., 2016). The ideal pH for phenol adsorption on cellulose and hydrochar is shown in Figure 4. With a value of 10.75 mg/g at pH 10, cellulose has the maximum adsorption capability. Hydrochar, on the other hand, reaches its maximal adsorption capability at pH 6, with a value of 12.74 mg/g. These data suggest that the ideal pH values for adsorption differ between cellulose and hydrochar, highlighting the impact of pH on the phenol adsorption capabilities of these materials.

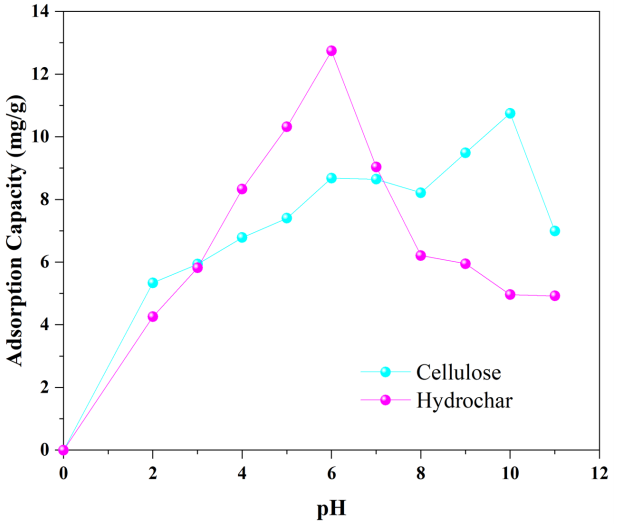

Figure 4. Effect of pH Adsorption by Cellulose and Hydrochar

The influence of contact time was used to find the best circumstances at different times. Table 1 shows the findings from the PSO and PFO adsorbent kinetics models for adsorbing phenol. The kinetics data analysis demonstrates that the PSO kinetics model's linear regression value (R^2) is closer to 1. This implies that phenol adsorption on PSO adsorbents follows the PSO kinetics model. Adsorption happens chemically, according to the PSO kinetics model, with the rate of adsorption determined by the content of both the adsorbent and the adsorbate (Priatna et al., 2023; Gao et al., 2022).

Figure 5 depicts the correlation between adsorption time and the quantity of phenol adsorbed on the cellulose adsorbent. Conversely, Figure 6 illustrates the corresponding graph for the hydrochar adsorbent, displaying the relationship between adsorption time and the amount of phenol adsorbed. These figures provide a visual representation of how the adsorption of phenol varies over time for each respective adsorbent.

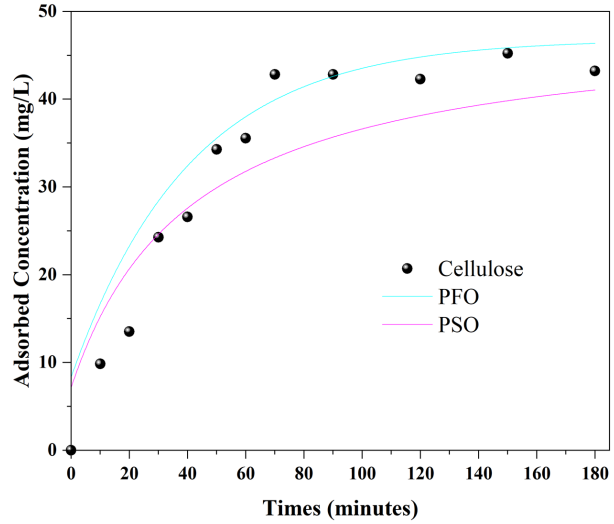

Figure 5. PFO and PSO Kinetic Model of Cellulose

As seen from Figures 5 and 6, the longer the contact time, the more phenol is absorbed until it reaches a point with optimum conditions so that the graph becomes linear. The optimum condition for cellulose adsorbent occurs at the 180^{th} minute, resulting in an absorbed phenol concentration of 43.209 mg/L. Similarly, the best condition for the hydrochar adsorbent is found during the 180^{th} minute, with an absorbed phenol concentration of 49.09 mg/L. These results show that the maximal phenol adsorption capacity is obtained at the stipulated time point for both cellulose and hydrochar adsorbents.

The Langmuir isotherm is often used to explain adsorption reactions that entail the creation of a monolayer and interactions between adsorbate molecules. The Langmuir isotherm hypothesis posits that adsorption occurs on a homogenous surface with no interaction between adsorbate molecules. Adsorption is described as a monolayer process with a restricted number of active sites on the adsorbent surface. The Freundlich isotherm theory, on the other hand, is applied to adsorption processes that involve several layers with little interaction between the adsorbate molecules. It views adsorption to be a multilayer process that occurs on a heterogeneous surface with several active sites. The Freundlich isotherm equation incorporates an empirical component that indicates adsorption capacity and intensity. It is used to describe adsorption on heterogeneous surfaces and is

Table 1. PFO and PSO Kinetic Model of Cellulose Cellulose and Hydrochar

Adsorbents	Qe_{exp} (mg/g)	PFO			PSO		
		Qe_{calc} (mg/g)	k_1 (min^{-1})	R^2	Qe_{calc} (mg/g)	k_2 (g/mg.min)	R^2
Cellulose	43.209	54.150	0.044	0.767	57.143	0.0004	0.955
Hydrochar	49.091	25.751	0.019	0.641	52.356	0.0012	0.986

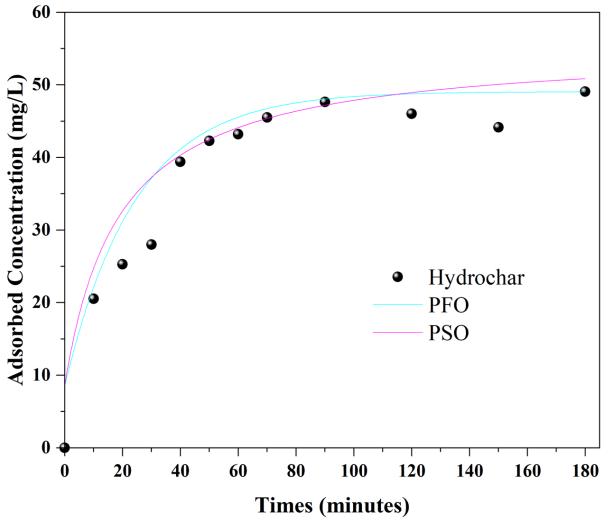

Figure 6. PFO and PSO Kinetic Model of Hydrochar

based on the assumption that adsorption happens via localized adsorption sites with changing adsorption energies. In conclusion, the Langmuir isotherm is well-suited for systems in which adsorption occurs in a monolayer and there are molecular interactions between adsorbate molecules. It presupposes a uniform surface with a restricted number of active spots. The Freundlich isotherm, on the other hand, is more relevant to multi-layer adsorption systems when there is no significant contact between the adsorbate molecules. It takes into account a heterogeneous surface with a distributed distribution of active sites. An empirical parameter that accounts for adsorption capacity and intensity is included in the Freundlich isotherm equation (Liu et al., 2021). The adsorption isotherms for cellulose and hydrochar are shown in Table 2. The high linear regression coefficient (R^2) values for the Freundlich isotherm equation for both adsorbents show a tendency to follow the Freundlich isotherm. This shows that the adsorption process on cellulose and hydrochar involves numerous layers and that the adsorbate molecules do not interact significantly. At a temperature of 60°C, the cellulose adsorbent reached its maximum adsorption capacity of 35.336 mg/g. The hydrochar adsorbent, on the other hand, displayed the highest adsorption capacity at 30°C, with a value of 21.008 mg/g. These data suggest that temperature has a major impact on the phenol adsorption capabilities of cellulose and hydrochar, and that ideal circumstances vary.

Table 3 shows the thermodynamic characteristics of phenol adsorption, which are determined from adsorption capacity data fluctuations in concentration and temperature. The free energy change (ΔG), entropy change (ΔS), and enthalpy change (ΔH) are among these parameters. These parameters' values provide useful information on the energetics and spontaneity of the adsorption process. By analyzing these thermodynamic parameters, researchers can assess the feasibility and thermodynamic nature of the phenol adsorption on the respective adsorbents (cellulose and hydrochar) under different conditions. The entropy value (ΔS) is also said to be the degree of disorder explaining the degree of disorder increases with increasing entropy value. entropy has a value of zero so that the reaction runs regularly which is concluded without any significant disturbance (Mahmoud, 2022). Gibbs free energy (ΔG) describes the spontaneity with which the reaction proceeds. A positive Gibbs free energy (ΔG) value explains the reaction is not spontaneous, vice versa (Ali et al., 2022).

An effective adsorbent should exhibit high adsorption capacity, fast adsorption rate, efficient separation and recovery capabilities, and high selectivity towards a wide range of elements or substances. These properties are crucial for ensuring successful and efficient removal or separation processes in various applications (Al-Ghouti et al., 2023). The ability to reuse an adsorbent is a crucial factor in making an adsorption process economically viable. This indicates that the adsorbent is capable of being regenerated and used for multiple cycles without experiencing any degradation in its performance. This not only reduces the cost associated with replacing the adsorbent but also enhances the sustainability and efficiency of the overall adsorption process. By ensuring the longevity and effectiveness of the adsorbent through multiple cycles, the economic feasibility of the adsorption process is significantly improved (Kumar et al., 2018).The cellulose and hydrochar adsorbents underwent a reuse test to assess their potential for multiple cycles of phenol adsorption. After the first use and each subsequent cycle, the adsorbents were separated from the phenol solution using an ultrasonic system. The separated adsorbents were then used repeatedly until the limit cannot be reused. The amount of phenol adsorbed was analyzed after each cycle to evaluate the effectiveness and capacity of the adsorbents for repeated usage. Based on the obtained data, it can be observed in Figure 7 that both cellulose and hydrochar adsorbents can be reused multiple times, up to 5 cycles, without a significant decline in their adsorption performance. This suggests that these adsorbents possess the ability to maintain their effectiveness and can be employed repeatedly, offering a cost-effective and sustainable solution for

Table 2. Isotherm Parameter Adsorption of Phenol

Adsorbent	T (°C)	Langmuir isotherm			Freundlich isotherm		
		Q_{max}	kL	R^2	n	kF	R^2
Cellulose	30	21.413	0.018	0.8574	1.191	1.905	0.9466
	40	20.450	0.014	0.8285	1.405	3.187	0.9594
	50	34.722	0.008	0.446	0.511	1.401	0.9847
	60	35.336	0.006	0.6886	2.002	7.084	0.9202
Hydrochar	30	21.008	0.036	0.6816	1.345	1.009	0.8955
	40	19.531	0.047	0.8232	1.451	1.245	0.9173
	50	17.007	0.068	0.9185	1.648	1.655	0.9234
	60	17.606	0.072	0.9224	1.665	1.795	0.9230

Table 3. Thermodynamic Parameter Adsorption of Phenol

Adsorbent	Concentration (mg/L)	ΔH (kJ/mol)	ΔS (kJ/mol)	ΔG (kJ/mol)			
				303 K	313 K	323 K	333 K
Cellulose	60	5,404	0,016	-10,344	-10.507	-10.670	-10.833
Hydrochar	30	5,680	0,011	2,335	2,224	2,114	2,004

phenol removal or other relevant applications.

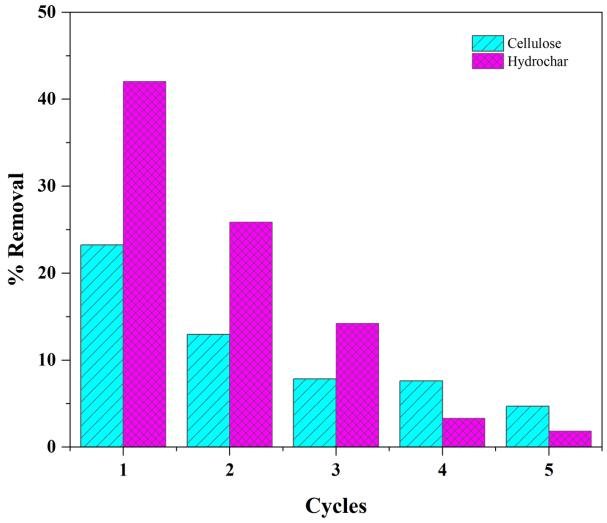

Figure 7. Regeneration Study of Cellulose and Hydrochar

4. CONCLUSIONS

Cellulose and hydrochar adsorbents were successfully synthesized and characterized using XRD, FT-IR, and BET analysis, providing insights into their structural and surface properties. The adsorption kinetics of both cellulose and hydrochar followed the pseudo-second order (PSO) model, suggesting a chemically-driven adsorption process. The adsorption isotherms of cellulose and hydrochar exhibited a good fit to the Freundlich model, indicating a multilayer adsorption mechanism with no significant adsorbate molecule interaction. The maximum adsorption capacity was determined to be 35.336 mg/g for cellulose and 21.008 mg/g for hydrochar, highlighting their potential as effective adsorbents for phenol removal. Furthermore, the cellulose and hydrochar adsorbents demonstrated the ability to be reused for up to five cycles of phenol adsorption, showcasing their reusability and potential for sustainable applications.

5. ACKNOWLEDGEMENT

Authors thank basecamp team for discussion and fruitfull comments regarding research work and this manuscript.

REFERENCES

Afifah, D. N., K. Riyani, T. Setyaningtiyas, Y. R. Hasanah, and A. Mufarij (2022). The Treatment of Phenol in Batik Wastewater by TiO_2-Copper Oxide (CuO And Cu_2O) Photocatalyst. *Jurnal Kartika Kimia*, **5**(1); 44–50

Al-Ghouti, M. A., M. Y. Ashfaq, M. Khan, Z. Al Disi, D. A. Da'na, and R. Shoshaa (2023). State-of-the-Art Adsorption and Adsorptive Filtration Based Technologies for the Removal of Trace Elements: A Critical Review. *Science of the Total Environment*, **895**; 164854

Ali, N. S., N. M. Jabbar, S. M. Alardhi, H. S. Majdi, and T. M. Albayati (2022). Adsorption of Methyl Violet Dye Onto a Prepared bio-Adsorbent from Date Seeds: Isotherm, Kinetics, and Thermodynamic Studies. *Heliyon*, **8**(8)

Atykyan, N., V. Revin, and V. Shutova (2020). Raman and FT-IR Spectroscopy Investigation the Cellulose Structural Differences from Bacteria Gluconacetobacter Sucrofermentans During the Different Regimes of Cultivation on a Molasses Media. *AMB Express*, **10**(1); 1–11

Chaari, I., A. Touil, and M. Medhioub (2021). Adsorption-Desorption of Phenolic Compounds from Olive Mills Wastewater Using Tunisian Natural Clay. *Chinese Journal of Chemical Engineering*, **40**; 287–292

da Silva, M. C., C. Schnorr, S. F. Lütke, S. Knani, V. X. Nascimento, É. C. Lima, P. S. Thue, J. Vieillard, L. F. Silva, and G. L. Dotto (2022). KOH Activated Carbons from Brazil Nut Shell: Preparation, Characterization, and Their Application in Phenol Adsorption. *Chemical Engineering Research and Design*, **187**; 387–396

de Farias, M. B., P. Prediger, and M. G. A. Vieira (2022). Conventional and Green-Synthesized Nanomaterials Applied for the Adsorption and/or Degradation of Phenol: A Recent Overview. *Journal of Cleaner Production*, **367**; 132980

Dehmani, Y., D. S. Franco, J. Georgin, T. Lamhasni, Y. Brahmi, R. Oukhrib, H. B. Youcef, and A. Sadik (2023a). Towards Experimental and Theoretical Understanding of the Adsorption Behavior of Phenol on a New Activated Carbon Prepared from Oak Wood. *Journal of Water Process Engineering*, **54**; 103936

Dehmani, Y., M. Mobarak, R. Oukhrib, A. Dahbi, A. Mohsine, T. Lamhasni, Y. Tahri, H. Ahlafi, S. Abouarnadasse, and E. C. Lima (2023b). Adsorption of Phenol by a Moroccan Clay/Hematite Composite: Experimental Studies and Statistical Physical Modeling. *Journal of Molecular Liquids*, **386**; 122508

El Hassani, K., B. H. Beakou, D. Kalnina, E. Oukani, and A. Anouar (2017). Effect of Morphological Properties of Layered Double Hydroxides on Adsorption of Azo Dye Methyl Orange: A Comparative Study. *Applied Clay Science*, **140**; 124–131

Fang, X., L. Gan, L. Wang, H. Gong, L. Xu, Y. Wu, H. Lu, S. Han, J. Cui, and C. Xia (2021). Enhanced Degradation of Bisphenol A by Mixed ZIF Derived CoZn Oxide Encapsulated N-Doped Carbon Via Peroxymonosulfate Activation: The Importance of N Doping Amount. *Journal of Hazardous Materials*, **419**; 126363

Gao, M., X. Wang, C. Xia, N. Song, Y. Ma, Q. Wang, T. Yang, S. Ge, C. Wu, and S. S. Lam (2021). Phenol Removal Via Activated Carbon from Co-Pyrolysis of Waste Coal Tar Pitch and Vinasse. *Korean Journal of Chemical Engineering*, **38**; 64–71

Gao, W., Z. Lin, H. Chen, S. Yan, H. Zhu, H. Zhang, H. Sun, S. Zhang, S. Zhang, and Y. Wu (2022). Roles of Graphitization Degree and Surface Functional Groups of N-Doped Activated Biochar for Phenol Adsorption. *Journal of Analytical and Applied Pyrolysis*, **167**; 105700

Kumar, P. S., W. W. Ejerssa, C. C. Wegener, L. Korving, A. I. Dugulan, H. Temmink, M. C. van Loosdrecht, and G.-J. Witkamp (2018). Understanding and Improving the Reusability of Phosphate Adsorbents for Wastewater Effluent Polishing. *Water Research*, **145**; 365–374

Liu, X., Y. Tu, S. Liu, K. Liu, L. Zhang, G. Li, and Z. Xu (2021). Adsorption of Ammonia Nitrogen and Phenol Onto the Lignite Surface: An Experimental and Molecular Dynamics Simulation Study. *Journal of Hazardous Materials*, **416**; 125966

Mahmoud, A. S. (2022). Effect of Nano Bentonite on Direct Yellow 50 Dye Removal; Adsorption Isotherm, Kinetic Analysis, and Thermodynamic Behavior. *Progress in Reaction Kinetics and Mechanism*, **47**; 14686783221090377

Mohammad, M., M. Mahmoud, and A. Afaj (2016). Study of Some Effecting Factors on the Removal of Phenol from Aqueous Solutions by Adsorption Onto Activated Carbon. *Journal of International Environmental Application and Science*, **11**(2); 148–153

Montoya-Escobar, N., D. Ospina-Acero, J. A. Velásquez-Cock, C. Gómez-Hoyos, A. Serpa Guerra, P. F. Gañan Rojo, L. M. Vélez Acosta, J. P. Escobar, N. Correa-Hincapié, and O. Triana-Chávez (2022). Use of Fourier Series in X-Ray Diffraction (XRD) Analysis and Fourier-Transform Infrared Spectroscopy (FTIR) for Estimation of Crystallinity in Cellulose from Different Sources. *Polymers*, **14**(23); 5199

Peyrovi, M. H. and M. Abolhassanzadeh Parizi (2022). The Modification of the BET Surface Area by Considering the Excluded Area of Adsorbed Molecules. *Physical Chemistry Research*, **10**(2); 173–177

Priatna, S. J., Y. M. Hakim, S. Wibyan, S. Sailah, and R. Mohadi (2023). Interlayer Modification of West Java Natural Bentonite as Hazardous Dye Rhodamine B. *Science and Technology Indonesia*, **8**(2); 160–169

Sajid, M., M. K. Nazal, N. Baig, and A. M. Osman (2018). Removal of Heavy Metals and Organic Pollutants from Water Using Dendritic Polymers Based Adsorbents: A Critical Review. *Separation and Purification Technology*, **191**; 400–423

Siregar, P. M. S. B. N., A. Wijaya, J. P. Nduru, N. Hidayati, A. Lesbani, and R. Mohadi (2022). Layered Double Hydroxide/C (C= Humic Acid; Hydrochar) as Adsorbents of Cr(VI). *Science and Technology Indonesia*, **7**(1); 41–48

Utami, H. P., N. Ahmad, Z. A. Zahara, A. Lesbani, and R. Mohadi (2022). Green Synthesis of Nickel Aluminum Layered Double Hydroxide using Chitosan as Template for Adsorption of Phenol. *Science and Technology Indonesia*, **7**(4); 530–535

Yang, L., H. Wang, J. Sun, Y. Xu, P. Li, Y. Xu, and S. Wu (2021). Effects of Process Parameters on the Physicochemical Properties of Corn Stalk Hydrochar and the Removal of Alkali and Alkaline Earth Metals. *IET Renewable Power Generation*, **15**(7); 1397–1407

Yu, S., X. Yang, Q. Li, Y. Zhang, and H. Zhou (2023). Breaking the Temperature Limit of Hydrothermal Carbonization of Lignocellulosic Biomass by Decoupling Temperature and Pressure. *Green Energy & Environment*, **8**(4); 1216–1227

Zhang, B., R. Zhao, D. Sun, Y. Li, and T. Wu (2019). Sustainable Fabrication of Graphene Oxide/Manganese Oxide Composites for Removing Phenolic Compounds by Adsorption-Oxidation Process. *Journal of Cleaner Production*, **215**; 165–174

Zulfajri, M., Y. T. Kao, and G. G. Huang (2021). Retrieve of Residual Waste of Carbon Dots Derived from Straw Mushroom as a Hydrochar for the Removal of Organic Dyes from Aqueous Solutions. *Sustainable Chemistry and Pharmacy*, **22**; 100469

